

PUBLICATION I

**Explicit treatment of thermal motion in
continuous-energy Monte Carlo
tracking routines**

Nucl. Sci. Eng., **171**, pp. 165–173.
Copyright 2012 by the American Nuclear Society.
Reprinted with permission from the publisher.

Explicit Treatment of Thermal Motion in Continuous-Energy Monte Carlo Tracking Routines

Tuomas Viitanen* and Jaakko Leppänen

VTT Technical Research Centre of Finland
P.O. Box 1000, FI-02044 VTT, Finland

Received June 6, 2011

Accepted October 11, 2011

Abstract—This paper introduces a new stochastic method for taking the effect of thermal motion into account on the fly in a Monte Carlo neutron transport calculation. The method is based on explicit treatment of the motion of target nuclei at collision sites and, consequently, requires simply cross sections at a temperature of 0 K regardless of the number of temperatures in the problem geometry. It utilizes rejection sampling techniques to manage the fact that total cross sections become distributed quantities. The method has a novel capability of accurately modeling continuous temperature distributions.

The new stochastic method is verified using a simple test program, which compares its results to an analytical reference solution based on NJOY-broadened cross sections. Future implementation to Monte Carlo reactor physics code *Serpent* is also discussed shortly.

I. INTRODUCTION

Material temperature plays an important role in nuclear reactor analysis, as all reaction rates are affected by the thermal motion of nuclides in the medium. Temperature effects cannot be neglected in any application without inflicting serious errors in the results, but their role is particularly emphasized in coupled neutronics/thermal hydraulics calculations dealing with heat transfer and feedback between fission power and coolant flow. These applications are becoming increasingly important for continuous-energy Monte Carlo codes as well, along with the development of computer capacity.

The traditional approach to dealing with the temperature effects involves using pregenerated, Doppler-broadened cross sections. This approach is well sufficient for applications where materials are at constant temperature or where the distributions can be approximated by constant effective values. More rigorous description of temperature gradients requires dividing the materials into several homogeneous subregions, each assigned with a different set of cross sections. This, in turn, requires additional storage space, which may become a practical

limitation if the number of subregions and nuclides is large.

One possibility to treat temperature distributions without excessive storage space requirements is to use interpolation between tabulated values.¹ This approach, however, requires relatively narrow spacing between the temperature points to reduce the interpolation errors to an acceptable level. The capability to use 0 K cross sections is another option that has been studied extensively within the past few years. Yesilyurt et al. have developed an efficient on-the-fly Doppler-broadening routine, based on series expansions and the multilevel Adler-Adler resonance representation.² Becker et al. have used another approach, relying on a stochastic algorithm for calculating effective integral and double-differential cross sections, which were utilized in the confirmation of the analytic scattering kernel.³

This paper presents another stochastic method for performing temperature corrections on reaction rates during the Monte Carlo transport simulation. The basic idea is very similar to Becker's method, but instead of performing stochastic Doppler broadening on the cross sections, the thermal motion of target nuclides is handled explicitly by making a coordinate transformation to target-at-rest frame (T-frame) at each collision point. The fact

*E-mail: tuomas.viitanen@vtt.fi

that material total cross sections become distributed quantities is handled using a rejection sampling routine on the neutron path lengths. As an additional feature, the use of this method also removes the homogeneity requirement and allows the modeling of continuous temperature distributions without approximations.

The current version of the method is unable to utilize the thermal scattering laws for bound atoms at thermal energies or probability table treatment at the unresolved resonance region, which somewhat limits the usability of the method in practical reactor calculations. The explicit treatment method also slightly complicates the implementation of flux estimators.

This paper considers only transport in a homogeneous material region with heterogeneous temperature, which is the simplest case that provides for proper verification of the method. However, the method can be straightforwardly generalized to transport in heterogeneous systems.

The methodology used in the calculation routines is introduced in Sec. II and demonstrated in Sec. III. The future implementation of the new method in the Serpent Monte Carlo code is discussed in Sec. IV, and Sec. V is left for the conclusions.

II. METHODS

The core of every Monte Carlo neutron transport code is the tracking routine, which simulates the random walk process by transporting neutrons through the geometry from one interaction to the next. The simulation is based on the fact that the free path length between two collision points is exponentially distributed, with the well-known probability density function (PDF) of the form

$$f(E, x) = \Sigma_{\text{tot}}(E) e^{-x \Sigma_{\text{tot}}(E)}, \quad (1)$$

where Σ_{tot} is the macroscopic total cross section of the medium. The conventional approach to sampling neutron path lengths from this distribution is to use the inversion method, which requires calculating the cumulative distribution function (CDF) of Eq. (1),

$$F(E, x) = \int_0^x f(E, x') dx' = 1 - e^{-x \Sigma_{\text{tot}}(E)}, \quad (2)$$

and using the inverse of the CDF with a uniformly distributed random variable ξ on the unit interval as a sample from f :

$$x = F^{-1}(E, \xi) = -\frac{1}{\Sigma_{\text{tot}}(E)} \ln(1 - \xi). \quad (3)$$

The prerequisite of this technique is that the total cross section remain constant throughout the path. If this is not the case, the integration in Eq. (2) does not hold, and the sample in Eq. (3) is not statistically valid. This happens,

for example, when the sampled collision point lies outside the material boundaries, in which case the neutron is stopped at the boundary surface and a new path length is sampled using the total cross section of the next material. The same limitation requires the geometry to be defined using homogeneous material regions without internal spatial variation in the total cross section.

II.A. Rejection Techniques for Sampling Neutron Path Length

It is important to notice that material homogeneity is a demand resulting from the use of the inversion sampling technique and not a characteristic of the Monte Carlo method itself. The limitation can be easily lifted by using rejection sampling techniques,⁴ which are based on the use of two distribution functions: the original PDF and a majorant function satisfying

$$f_{\text{maj}}(z) \geq f(z) \quad (4)$$

for all values of the random variable and formed in such a way that values from f_{maj} can be sampled using the inversion method. According to the theory, values sampled from the majorant function and accepted with probability

$$P = \frac{f(z)}{f_{\text{maj}}(z)} \quad (5)$$

follow the distribution of f . Rejected values are discarded, and the procedure is repeated until a successful sample is obtained from Eq. (5).

A good example of using rejection techniques for sampling neutron path lengths is the Woodcock delta-tracking method,⁵ which allows the random walk to be continued over one or several material boundaries without stopping the track at each boundary surface. The free path length is sampled using Eq. (3), with material total cross section replaced by the majorant cross section:

$$\Sigma_{\text{maj}}(E) \geq \Sigma_{\text{tot}}(E, x). \quad (6)$$

The collision point is accepted with probability

$$P(E, x) = \frac{\Sigma_{\text{tot}}(E, x)}{\Sigma_{\text{maj}}(E)}. \quad (7)$$

If the point is rejected, the procedure is restarted by sampling a new path length using the majorant cross section.

This study deals with a very similar problem. Material total cross sections are not constant, but instead of discrete discontinuities at boundary crossings, the values are characterized by a continuous distribution. The variation in the value of Σ_{tot} results from the fact that reaction cross sections are evaluated in the T-frame at energy E' , which depends not only on the neutron energy E in the laboratory frame (L-frame), but also on the thermal motion of the target nucleus. The rejection sampling

routine applied to the problem accounts for this variation by using a majorant cross section for sampling the neutron path lengths. Similar to in delta tracking, the actual value of Σ_{tot} is needed only at the tentative collision points. In delta tracking this value depends on the material where the collision occurs. In this case the velocity of the target nucleus is sampled from a Maxwellian-based distribution to make a transfer from L-frame to T-frame, and the result dictates the energy at which cross section is evaluated.

It should be noted that the explicit temperature treatment method only governs the way neutrons are transported inside a material region. Thus, the method is applicable to all kinds of tracking schemes including delta and surface tracking. As an additional remark, the track-length estimators—usually utilized with surface tracking—can only be used to calculate integrals of quantities that are homogeneous inside a material zone. Therefore, for example, reaction frequencies inside a region with an inhomogeneous temperature profile must be calculated using collision estimators. This is a limitation of the track-length estimator, not of the explicit temperature treatment itself.

II.B. Forming the Majorant Cross Section

The majorant cross section must be defined in such a way that the value is always greater than or equal to the T-frame total cross section at the collision point:

$$\Sigma_{\text{maj}}(E) \geq \Sigma_{\text{tot}}^0(E', x) , \tag{8}$$

where the superscript indicates that the cross sections are generated at absolute zero temperature. Since the T-frame energy is a distributed quantity, finding the maximum value requires determining the variation of relative velocity $v' \in [v'_{\text{min}}, v'_{\text{max}}]$, corresponding to relative energy E' , as a function of L-frame velocity v , material temperature T , and nuclide mass $m = AM_n$.

If the velocity of the target nucleus equals V_t , the maximum of

$$v' = \sqrt{v^2 + V_t^2 - 2vV_t\mu} \tag{9}$$

corresponds to a parallel collision with $\mu = -1$. Relative velocity v' is minimal for a head-on collision with $\mu = 1$ unless $V_t > v$, in which case the velocity may reach arbitrarily small values. Thus,

$$v'_{\text{max}} = v + V_t \tag{10}$$

and

$$v'_{\text{min}} = \begin{cases} v - V_t , & \text{if } V_t \leq v \\ 0 \approx v_0 , & \text{if } V_t > v , \end{cases} \tag{11}$$

where v_0 corresponds to the lowest energy in the cross-section energy grid.^a

Both of the extremities are obtained with the highest possible value of V_t . Target velocity V_t is assumed to obey the Maxwell-Boltzmann distribution

$$P_{\text{MB}}(V_t) = \frac{4}{\sqrt{\pi}} \gamma^3 V_t^2 e^{-\gamma^2 V_t^2} \tag{12}$$

and

$$\gamma(T, A) = \sqrt{\frac{AM_n}{2kT}} , \tag{13}$$

where k is the Boltzmann constant. To be precise, this assumption is only valid for ideal gases, not for example crystalline materials like UO_2 . Hence, the sampling of target velocities from the Maxwell-Boltzmann distribution may cause bias in the results. This issue, however, concerns not only the current study but also many other calculation codes in which this very common assumption is made. For instance, all effective cross sections broadened by the SIGMA1 code (used in NJOY) have the same assumption built in.⁶

Since the distribution (12) has an infinite tail, it is impossible to determine an unambiguous maximum for the velocity, and therefore, an approximation must be introduced. If the approximative maximum is chosen too high, Σ_{maj} becomes inefficiently conservative, while too-small values may result in significant errors.

A convenient way of dealing with a similar problem was introduced in the SIGMA1 module of NJOY (Ref. 7) and was recently utilized in the creation of a majorant cross section for the Doppler broadening rejection correction method by Becker et al.⁸ In SIGMA1, a target velocity of

$$V_t = \frac{4}{\gamma(T, A)} \tag{14}$$

was used as a cutoff value in the integrals of the Doppler-broadening algorithm. The same cutoff value is adopted as the maximum of V_t in the current study also. This approximation omits a proportion of 5×10^{-7} of the most energetic nuclei, which is considered a suitable compromise between efficiency and accuracy. For the majorant to be conservative, the temperature T in Eq. (13) must be chosen as the maximum T_{max} inside a material region in the case of nonuniform temperature distributions.

^aPhysically correct cross-section extrapolation to zero velocity would result in an unfeasible, infinite majorant in the case of $1/v$ -shaped cross sections. Hence, cross sections for $v' \leq v_0$ are approximated with $\Sigma_{\text{tot}}(v_0)$ when forming the majorant. The effect of this approximation was studied and found insignificant.

To summarize the above discussion, Σ_{maj} for neutron energy E is obtained as the maximum of the 0 K total cross section Σ_{tot}^0 within an interval $E' \sim v' \in [v'_{\text{min}}, v'_{\text{max}}]$ defined by Eqs. (10), (11), and (14).

II.C. Sampling Target Velocity

The tracking routine proceeds in the conventional way, the only difference being that the neutron path lengths are sampled using majorants instead of macroscopic total cross sections. Once the collision point x is reached, the T-frame energy E' is sampled based on distribution $P(V_t, \mu)$.

For the tracking routine to be consistent with the traditional transport methods relying on effective cross sections, it is obvious that the distribution $P(V_t, \mu)$ must satisfy relation

$$\iint \Sigma_i^0(v', x) P(V_t, \mu) dV_t d\mu = \Sigma_{\text{eff}}(v, x, T), \quad (15)$$

where $\Sigma_{\text{eff}}(v, x, T)$ is the effective cross section for temperature T , defined^{9,10}

$$\Sigma_{\text{eff}}(v, x, T) = \frac{1}{v} \iint v' \Sigma_i^0(v', x) P_{\text{MB}}(V_t) dV_t d\frac{\mu}{2}. \quad (16)$$

From Eqs. (15) and (16), it results that consistency is achieved if

$$P(V_t, \mu) = \frac{v'}{2v} P_{\text{MB}}(V_t), \quad (17)$$

which is exactly the same distribution that is used in the sampling of target velocities in the free gas thermal treatment of MCNP. Hence, also the sampling procedure is the same, as described in the following.

Because of the v' multiplier, direct sampling from the distribution Eq. (17) is problematic. Consequently, Eq. (17) is rewritten in the form

$$P(V_t, \mu) = C \left\{ \frac{v'}{v + V_t} \right\} \left\{ (2\gamma^4) V_t^3 e^{-\gamma^2 V_t^2} + B(4\gamma^3/\sqrt{\pi}) V_t^2 e^{-\gamma^2 V_t^2} \right\}, \quad (18)$$

where constants C and

$$B = \frac{\gamma v \sqrt{\pi}}{2} \quad (19)$$

are both independent of V_t . The nuclide velocity is sampled from $V^3 e^{-\gamma^2 V^2}$ distribution with probability $Q =$

$1/(1 + B)$ and from $V^2 e^{-\gamma^2 V^2}$ with probability $1 - Q$. The cosine between the velocity vectors is obtained from an isotropic distribution, and the sample is accepted with probability $v'/(v + V_t) \leq 1$. The sampling is repeated until an accepted v' is found.¹¹

II.D. Rejection Sampling at Collision Point

The procedure continues by rejection sampling using the 0 K total cross section at energy E' corresponding to the sampled relative velocity v' . The collision point x is accepted with probability

$$P = \frac{\Sigma_{\text{tot}}^0(E', x)}{\Sigma_{\text{maj}}(E)}. \quad (20)$$

If the point is rejected, the whole procedure restarts by sampling a new path length starting from x . The 0 K cross sections are also used for sampling the reaction mode. The probability of sampling reaction i is simply

$$P_i = \frac{\Sigma_i^0(E', x)}{\Sigma_{\text{tot}}^0(E', x)}. \quad (21)$$

II.E. Normalization Factor for Low Energies

The explicit treatment of target motion, as introduced above, cannot fully account for the low-energy effects on effective cross sections, namely, the increase in potential scattering rate when $E \ll kT$. As the energy of a neutron approaches zero, the thermal motion of the surrounding nuclei becomes an increasingly important cause for collision events. Thus, the slower the velocity of the neutron, the more thermal-motion-initiated collisions occur per traveled path length, and consequently, the larger the apparent increase in effective potential scattering cross section. This effect does not affect the fission and capture cross sections that typically behave as $1/v$ at low energies.

A mathematical explanation for this phenomenon is concealed in Eq. (17) or, more precisely, the fact that Eq. (17) is not actually a distribution in the sense that its integral over V_t and μ differs significantly from unity if $E \ll kT$. The value of this integral depends on the L-frame velocity of the incident neutron v and equals

$$g(v, T, A) = \iint \frac{v'}{2v} P_{\text{MB}}(V_t) d\mu dV_t = \left(1 + \frac{1}{2\gamma(T, A)^2 v^2} \right) \text{erf}(\gamma(T, A)v) - \frac{e^{-\gamma(T, A)^2 v^2}}{\sqrt{\pi} \gamma(T, A) v}, \quad (22)$$

which can be easily written also in terms of energy as $g(E, T, A)$ (Ref. 11).

Equation Eq. (17) is rewritten in the form

$$P(V_t, \mu) = g(v, T, A) P_1(V_t, \mu) , \quad (23)$$

where the integral of

$$P_1(V_t, \mu) = \frac{1}{g(v, T, A)} \frac{v'}{2v} P_{MB}(V_t) \quad (24)$$

equals unity for all v and, therefore, is the actual distribution used in the sampling of target velocity since only one nuclide is considered per collision. Taking this into account, Eq. (15) is corrected in accordance with the sampling procedure as

$$\begin{aligned} & \iint g(v, T, A) \Sigma_i^0(v', x) P_1(V_t, \mu) dV_t d\mu \\ &= \Sigma_{\text{eff}}(v, x, T) . \end{aligned} \quad (25)$$

Equation (25) points out that the low-energy phenomenon can be correctly accounted for by multiplying all the 0 K cross sections used in the transport simulation with factor $g(E, T, A)$. Correspondingly, the same correction must be applied also for the majorant cross sections with $T = T_{\text{max}}$, i.e.,

$$\Sigma_{\text{maj, corr}}(E) = g(E, T_{\text{max}}, A) \Sigma_{\text{maj}}(E) , \quad (26)$$

where Σ_{maj} is as defined in Sec. II.B.

II.F. Materials Consisting of Multiple Nuclides

Since the distribution of target velocity depends on nuclide mass, the procedure introduced in Secs. II.B through II.E cannot be directly applied to materials consisting of multiple nuclides. The simplest way to solve this problem is to form a material-wise majorant cross section by summing over the nuclide-wise majorants in the composition

$$\begin{aligned} \Sigma_{\text{maj, corr}}(E) &= \sum_n \Sigma_{\text{maj, corr, } n}(E) \\ &= \sum_n g(E, T_{\text{max}}, A_n) \Sigma_{\text{maj, } n}(E) . \end{aligned} \quad (27)$$

Neutron path lengths are sampled using $\Sigma_{\text{maj, corr}}$, and rejection sampling is divided into two parts. First, the target nuclide n is sampled with probability

$$P_n = \frac{\Sigma_{\text{maj, corr, } n}(E)}{\Sigma_{\text{maj, corr}}(E)} = \frac{g(E, T_{\text{max}}, A_n) \Sigma_{\text{maj, } n}(E)}{\Sigma_{\text{maj, corr}}(E)} . \quad (28)$$

This selection is then followed by the sampling of T-frame energy E' , rejection sampling with acceptance criterion

$$\xi < \frac{g(E, T(x), A_n) \Sigma_{\text{tot, } n}^0(E', x)}{g(E, T_{\text{max}}, A_n) \Sigma_{\text{maj, } n}(E)} , \quad (29)$$

and, finally, the reaction sampling using the 0 K cross sections

$$P_i = \frac{g(E, T(x), A_n) \Sigma_{i, n}^0(E', x)}{g(E, T(x), A_n) \Sigma_{\text{tot, } n}^0(E', x)} = \frac{\Sigma_{i, n}^0(E', x)}{\Sigma_{\text{tot, } n}^0(E', x)} . \quad (30)$$

III. DEMONSTRATION

The validity of the new method is demonstrated with a test program. It uses the methodology described in Sec. II to sample next collision sites and reactions for neutrons with user-defined L-frame energies E . To demonstrate the capability of heterogeneous temperature modeling, the test calculations are performed for a one-dimensional single-material system in which neutron paths begin from $x = 0$, region $x \leq x_0$ is at temperature T_1 , and region $x > x_0$ is at temperature T_2 .

Advantageous to the verification purpose, the neutron mean free path (mfp) can be analytically resolved in the chosen system. The mfp for a neutron with energy E is

$$\begin{aligned} l(E) &= \frac{1}{\Sigma_{\text{tot, } 1}(E)} \\ &+ e^{-\Sigma_{\text{tot, } 1}(E)x_0} \left(\frac{1}{\Sigma_{\text{tot, } 2}(E)} - \frac{1}{\Sigma_{\text{tot, } 1}(E)} \right) , \end{aligned} \quad (31)$$

where $\Sigma_{\text{tot, } 1}$ and $\Sigma_{\text{tot, } 2}$ are the Doppler-broadened total cross sections for temperatures T_1 and T_2 , respectively. The test program uses this result, together with reaction probabilities

$$\begin{aligned} P_i &= (1 - e^{-\Sigma_{\text{tot, } 1}(E)x_0}) \frac{\Sigma_{i, 1}(E)}{\Sigma_{\text{tot, } 1}(E)} \\ &+ e^{-\Sigma_{\text{tot, } 1}(E)x_0} \frac{\Sigma_{i, 2}(E)}{\Sigma_{\text{tot, } 2}(E)} , \end{aligned} \quad (32)$$

to provide analytical reference results. Sampling path lengths and reactions using the stochastic method should reproduce the same behavior with 0 K data, when the results are averaged over a large number of samples.

The medium in the test case consists of 8.3% enriched uranium oxide. Fuel material is at 900 K for $x \leq x_0$ and at 1800 K for $x > x_0$. Temperature boundary x_0 is at 0.0197 cm, which corresponds to the lethargy-averaged mfp at 900 K. The calculations were performed with JEFF-3.1-based cross-section data.

In the specific test case, the sampling efficiency of acceptance criterion Eq. (29) varied between 0.2% at an energy point in the resonance region (186 eV) to almost 100% at energies close to 1 MeV. The average efficiency was 41% when the energies E were chosen in 500 equi-lethargy intervals from 10^{-11} to 15 MeV.

Selected results are presented in Fig. 1. The results in Fig. 1 are calculated using a cross-section library processed with NJOY using 0.003 reconstruction tolerance. Ten million samples were run per each energy E .

Comparison of the results is carried out for neutron mfp and fission, capture, and elastic scattering

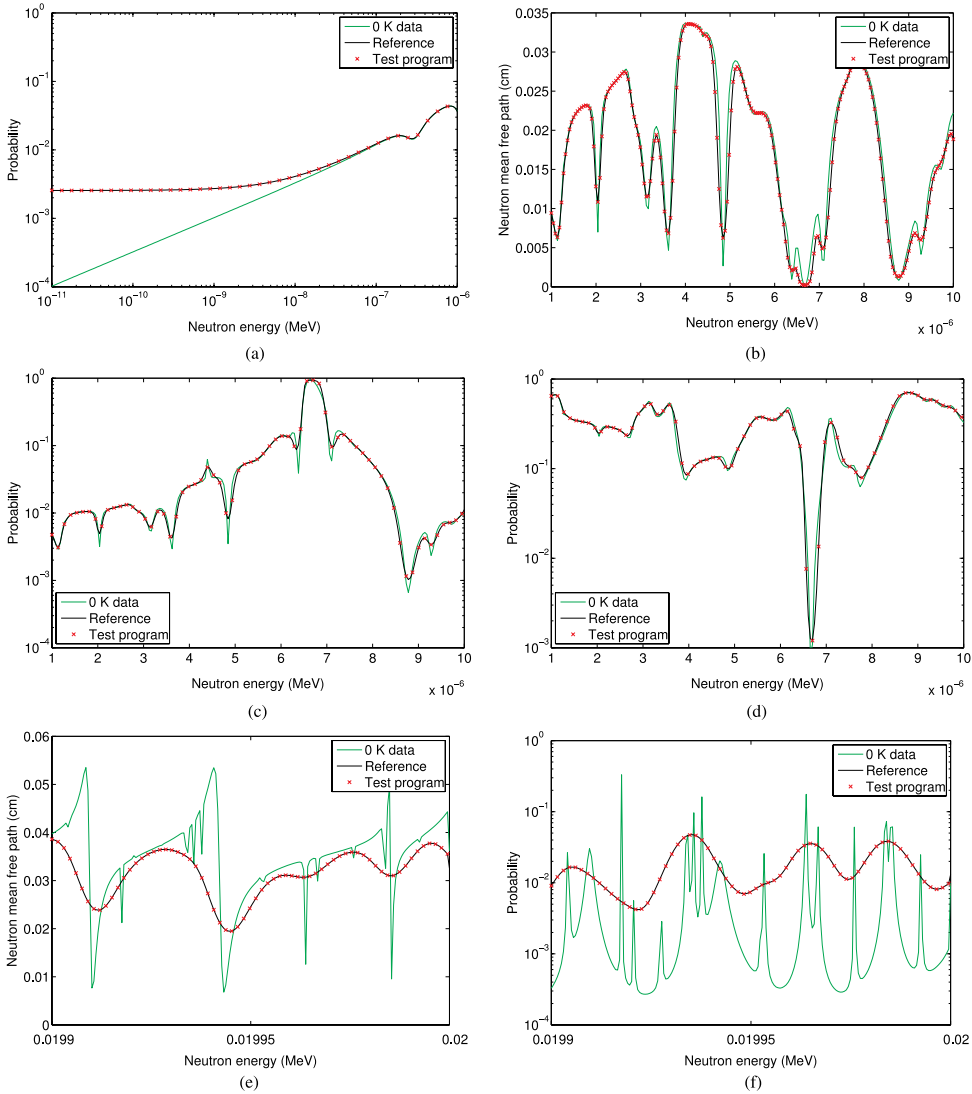


Fig. 1. The correspondence between the test routine and the NJOY-based reference results is excellent. (a) Elastic scattering probability of ^{16}O (thermal energy region). (b) Neutron mfp (low-resonance region). (c) Uranium-238 capture probability (low-resonance region). (d) Uranium-235 fission probability (low-resonance region). (e) Neutron mfp (high-resonance region). (f) Uranium-238 capture probability (high-resonance region).

probabilities of the uranium isotopes and ^{16}O . To distinguish the impact of thermal motion, analytical solutions are also provided at zero temperature. Three energy intervals are considered:

Thermal region: 1×10^{-11} to 1×10^{-6} MeV—This energy region lies below the first resonances and shows the low-energy behavior of elastic scattering cross sections.

Low resonance region: 1×10^{-6} to 1×10^{-5} MeV—This region covers the lowest resonance peaks of ^{235}U and ^{238}U .

High-resonance region: 19.9×10^{-3} to 20×10^{-3} MeV—This is the higher end of the resolved resonance region, just below unresolved resonances.

Neutron capture and fission are the dominant reaction modes at low energies. Since the cross sections of these reactions are unaffected by thermal motion, differences in neutron mfp remain small as well. Elastic scattering cross sections are increased, which is shown in the reaction probabilities. The curves for ^{16}O are plotted in Fig. 1a. The agreement is good and the differences clear when compared to 0 K data.

The low-resonance region covers the first high peak of ^{238}U and several lower humps of ^{235}U . The high capture resonance at 6.7 eV drops neutron mfp close to zero,

as seen in Fig. 1b. Broadening of the resonance peaks is clearly shown in the reaction probabilities, and the effect is well reproduced by the stochastic model.

Resonances in the high end of the resolved region exhibit strong overlap when broadened to 900 or 1800 K temperature. Neutron mfp and ^{238}U capture probability in Figs. 1e and 1f barely resemble the 0 K data. The analytical and stochastic results are in good agreement.

Test calculations were also performed for the whole energy spectrum using two cross-section libraries of different reconstruction tolerances, namely, 0.010 and 0.003. To minimize the statistical errors, the number of neutrons per energy grid point was increased to one hundred million. Relative differences in mfp are plotted in Fig. 2 for both of the libraries.

In Fig. 2, a small negative bias can be recognized at energies below 10^{-7} MeV. It originates from the limited accuracy of the cross-section representation in which the cross sections between energy grid points are obtained via linear interpolation. NJOY chooses the energy grid so that the proportional error of linear interpolation does not exceed the reconstruction tolerance.¹² In the resonance region of a typical cross-section curve, the linear interpolation results occasionally in both too-high and too-small values. Instead, when a $1/v$ -shaped cross-section curve is approximated with linear interpolation, the result is systematically larger than the actual cross section. Since the dominating fission and capture cross

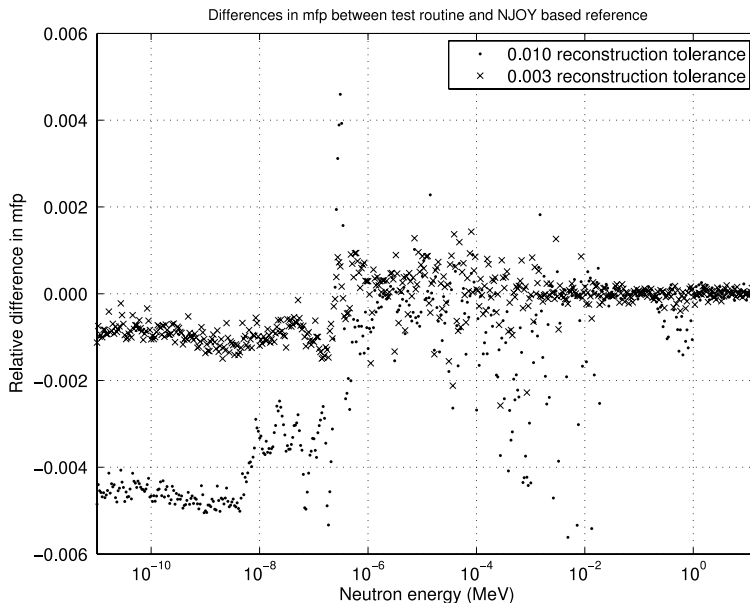


Fig. 2. The relative difference plot between the test routine and reference results points out a minor bias at thermal energies.

sections are $1/v$ -shaped at low energies, the total cross section becomes positively biased, which results in a negative bias in the mfp.

As can be seen in Fig. 2, the proportional deviances in mfp are smaller than the reconstruction tolerances. In other words, the limited accuracy of the cross-section representation, together with an insignificant amount of statistical error, accounts for all the perceived errors in mfp. Thus, the new explicit temperature treatment method seems just as accurate as the available cross-section libraries, at least when compared to an NJOY-based benchmark.

IV. FUTURE IMPLEMENTATION IN SERPENT

Serpent is a three-dimensional continuous-energy Monte Carlo neutron transport code, specifically developed for reactor physics calculations.^b The code uses multitemperature ACE format cross-section libraries that can be Doppler-broadened to an arbitrary temperature using a built-in preprocessor routine.^{13,14} This approach is considered sufficient for most of the present applications, typically related to group constant generation, burnup calculation, and research reactor modeling, in which the number of material temperatures is usually very limited. The main reason for this study was to develop a method that could extend the temperature treatment to an arbitrary number of temperatures, which is a requirement encountered in coupled neutronics/thermal hydraulics calculations and other multiphysics applications.

The theoretical basis and demonstration discussed in this paper show the viability of the new method, but the practical implementation still requires much work. In addition to the transport routine, the on-the-fly sampling of cross sections must be compatible with the methods used for calculating various reaction rate tallies, needed for group constant generation and burnup calculation. We are currently investigating the best practices for implementing these routines in the Serpent code. This, and the performance of the new method, remain topics for future studies.

V. SUMMARY AND CONCLUSIONS

A new stochastic method for performing Doppler broadening on the fly in a Monte Carlo transport simulation is introduced. The method is based on explicit treatment of target motion at collision sites. A collision point candidate x is first sampled using a majorant cross

section, the relative velocity of the collision nuclide to the incident neutron is sampled from a Maxwellian-based distribution, and finally, the collision point is accepted or rejected according to the 0 K cross section corresponding to the relative velocity. In case of a rejection the procedure restarts by sampling of a new path length starting from x .

The method is verified with a test program, which compares results of the stochastic algorithm to analytical reference results based on effective NJOY cross sections. The results of the algorithm are in good agreement with the reference. The minor differences between the results are recognized to originate from the finite accuracy of the reconstructed cross sections, not the method itself.

Sampling efficiency of the method varied substantially with neutron energy, but the average efficiency was a rather promising 41%. Nevertheless, no conclusions can be drawn on the practical efficiency or even feasibility of the method in a Monte Carlo transport routine before a thorough implementation in a transport code.

There are at least two significant advantages in the new method. First of all, as a common feature to all on-the-fly Doppler-broadening techniques including Ref. 2, merely 0 K cross-section libraries are required regardless of the number of different temperatures appearing in a problem geometry. Consequently, the processing and storage of cross-section libraries is reduced to one temperature. More importantly, only 0 K cross sections need to be stored in the computer memory during transport calculation, significantly decreasing the memory demand of multitemperature transport problems.

The second advantageous property is unique for the explicit temperature treatment method: It provides for accurate modeling of continuous temperature distributions. This property can be taken advantage of, for instance, in the verification of current methods used in the determination of effective fuel temperatures. The importance of accurate temperature modeling is also emphasized in coupled neutronics/thermal hydraulics and neutronics/fuel behavior calculations that are increasingly important applications for Monte Carlo reactor physics codes.

ACKNOWLEDGMENTS

This work was funded from the KÄÄRME project under the Finnish Research Programme on Nuclear Power Plant Safety SAFIR2014.

REFERENCES

1. T. H. TRUMBULL, "Treatment of Nuclear Data for Transport Problems Containing Detailed Temperature Distributions," *Nucl. Technology*, **156**, 75 (2006).

^bA complete and up-to-date description of the Serpent code is found at the project Web site: <http://montecarlo.vtt.fi> (current as of June 6, 2011).

2. G. YESILYURT, W. R. MARTIN, and F. B. BROWN, "On-the-Fly Doppler Broadening for Monte Carlo Codes," *Proc. M&C 2009*, Saratoga Springs, New York, May 3–7, 2009.
3. B. BECKER et al., "An Alternative Stochastic Doppler Broadening Algorithm," *Proc. M&C 2009*, Saratoga Springs, New York, May 3–7, 2009.
4. I. LUX and L. KOBLINGER, *Monte Carlo Particle Transport Methods: Neutron and Photon Calculations*, CRC Press (1991).
5. E. R. WOODCOCK et al., "Techniques Used in the GEM Code for Monte Carlo Neutronics Calculations in Reactors and Other Systems of Complex Geometry," ANL-7050, Argonne National Laboratory (1965).
6. D. E. CULLEN and C. R. WEISBIN, "Exact Doppler Broadening of Tabulated Cross Sections," *Nucl. Sci. Eng.*, **60**, 199 (1976).
7. D. E. CULLEN, "Program SIGMA1 (version 79-1): Doppler Broaden Evaluated Cross Sections in the Evaluated Nuclear Data File/Version B (ENDF/B) Format," UCRL-50400 Part B, Lawrence Livermore National Laboratory (1979).
8. B. BECKER, R. DAGAN, and G. LOHNERT, "Proof and Implementation of the Stochastic Formula for Ideal Gas, Energy Dependent Scattering Kernel," *Ann. Nucl. Energy*, **36**, 470 (2009).
9. E. P. WIGNER and J. E. WILKINS, Jr., "Effect of the Temperature of the Moderator on the Velocity Distribution of Neutrons with Numerical Calculations with H as Moderator," AECD-2275, Clinton Laboratory (1944).
10. A. W. SOLBRIG, Jr., "Doppler Effect in Neutron Absorption Resonances," *Am. J. Phys.*, **29**, 257 (1961).
11. MCNP X-5 MONTE CARLO TEAM, "MCNP—A General Monte Carlo N-Particle Transport Code," Version 5, LA-UR-03-1987, Los Alamos National Laboratory (2003).
12. R. E. MacFARLANE and D. W. MUIR, "NJOY99.0 Code System for Producing Pointwise and Multigroup Neutron and Photon Cross Sections from ENDF/B Data," PSR-480, Los Alamos National Laboratory (2000).
13. T. VIITANEN, "Implementing a Doppler-Preprocessor of Cross Section Libraries in Reactor Physics Code Serpent," M.Sc. Thesis, Helsinki University of Technology (2009).
14. J. LEPPÄNEN and T. VIITANEN, "New Data Processing Features in the Serpent Monte Carlo Code," *J. Korean Phys. Soc.*, **59**, 1365 (2011).